Arabian Journal of Chemistry (2017) xxx, xxx–xxx

King Saud University

Arabian Journal of Chemistry

www.ksu.edu.sa
www.sciencedirect.com

ORIGINAL ARTICLE

Synthesis and characterization of thin film composite membranes made of PSF-TiO_2/GO nanocomposite substrate for forward osmosis applications

T. Sirinupong [a,b], W. Youravong [a,b,*], D. Tirawat [a], W.J. Lau [c], G.S. Lai [c], A.F. Ismail [c]

[a] *Department of Food Technology, Faculty of Agro-Industry, Prince of Songkla University, 90110 Hat Yai, Thailand*
[b] *Membrane Science and Technology Research Center, Prince of Songkla University, 90110 Hat Yai, Thailand*
[c] *Advanced Membrane Technology Research Centre (AMTEC), Universiti Teknologi Malaysia, 81310 Skudai, Johor, Malaysia*

Received 14 February 2017; accepted 8 May 2017

KEYWORDS

Nanocomposite substrate;
TFC membrane;
TiO_2;
Graphene oxide;
Forward osmosis

Abstract Support layer of thin film composite (TFC) membrane plays an important role in forward osmosis (FO) performance. A new type of support layer or nanocomposite substrate was developed by incorporating titanium dioxide (TiO_2)/graphene oxide (GO) into polysulfone (PSF) matrix. Prior to performance evaluation, the developed substrates were characterized with respect to surface chemistry, roughness and cross-sectional morphology. The results showed that both surface hydrophilicity and roughness of PSF-based substrates were increased upon incorporation of nanomaterials. Substrates with long finger-like voids extended from the top to the bottom could be developed upon incorporation of TiO_2 ($Substrate_{TiO_2}$) or TiO_2/GO mixture ($Substrate_{TiO_2/GO}$). The improved surface hydrophilicity and favorable structure formed are the main factors leading to higher water flux of nanocomposite substrate. Moreover, the water flux of FO using TFC membranes could be enhanced using this nanocomposite substrate. Comparing to the control TFC membrane, the TFC membranes made of $Substrate_{TiO_2}$ and $Substrate_{TiO_2/GO}$ exhibited greater water flux with minimum increase in reverse draw solute flux. Based on the results obtained, it can

* Corresponding author at: Department of Food Technology, Faculty of Agro-Industry, Prince of Songkla University, 90110 Hat Yai, Thailand.
E-mail address: wirote.y@psu.ac.th (W. Youravong).

Peer review under responsibility of King Saud University.

Production and hosting by Elsevier

http://dx.doi.org/10.1016/j.arabjc.2017.05.006

Please cite this article in press as: Sirinupong, T. et al., Synthesis and characterization of thin film composite membranes made of PSF-TiO_2/GO nanocomposite substrate for forward osmosis applications. Arabian Journal of Chemistry (2017), http://dx.doi.org/10.1016/j.arabjc.2017.05.006

be concluded that the incorporation of TiO_2 and/or GO nanoparticles into PSF substrate could potentially improve the TFC membrane performance during FO applications.

1. Introduction

Nowadays, forward osmosis (FO) which is an osmotically driven membrane process obtains much attention worldwide as an alternative process for brackish water and seawater desalination (Chung et al., 2011; Shaffer et al., 2012), liquid food concentration (Nayak and Rastogi, 2010) and power generation (Kim and Elimelech, 2013). Since the permeate flux, a key performance indicator of FO is induced by the osmotic pressure difference between the feed and the draw solutions, an external driving force is therefore not required. Furthermore, FO offers high contaminants rejection and low membrane fouling compared with reverse osmosis (RO), an external pressure-driven process (Cornelissen et al., 2008). However, the industrial implementation of FO has been hindered by the lack of ideal membrane properties, i.e., low support layer resistance of water transport, high water permeability, minimum reverse solute permeability, excellent mechanical properties and wide range of pH tolerance (Tiraferri et al., 2012; Widjojo et al., 2013).

A thin film composite (TFC) membrane made of interfacial polymerization technique is widely used for FO. It has a unique structure as both top selective layer and bottom support layer could be flexibly manipulated to achieve desirable properties (Lau et al., 2015). In comparison to the TFC membrane used for RO and nanofiltration (NF) processes, the properties of support layer are more important in FO process. During FO process, both sides (selective layer and support layer) of TFC membrane are simultaneously contacted with feed and draw solutions. In this case, support layer is as important as selective layer (Emadzadeh et al., 2016; Lai et al., 2016a, 2016b). The ideal properties of support layer should be thin, highly porous and low tortuosity in order to achieve desirable performance for FO process.

The support layer of TFC membrane is usually made of semi-hydrophobic polymers such as polysulfone (PSF) and polyethersulfone (PES) with water contact angle falls in the range of 65–75° (Han et al., 2012; Sahebi et al., 2016). For FO membrane, the support layer should be as hydrophilic as possible in order to attain maximum surface wettability and mitigate internal concentration polarization (ICP). To achieve this desirable property, the approach of incorporating hydrophilic nanomaterial into the polymeric substrate was attempted. Previous works have demonstrated that the incorporation of hydrophilic nanoparticles such as titanium dioxide (TiO_2) (Emadzadeh et al., 2014), silica dioxide (SiO_2) (Liu and Ng, 2015), halloysite nanotube (HNTs) (Zhu et al., 2014), carbon nanotube (CNTs) (Son et al., 2015) and graphene oxide (GO) (Lai et al., 2016a, 2016b) could improve not only the support layer or substrate hydrophilicity but also its morphology which is related to the structural (S) parameter (Deshmukh et al., 2015). For example, the incorporation of multiwall carbon-nanotubes (MWCNTs) into PSF-based membrane could decrease water contact angle and improve water flux by 60–100%, depending on the loading used (Yin et al., 2013). Likewise, the incorporation of appropriate amount of SiO_2 nanoparticle into the PSF matrix could improve the substrate wettability and reduced S parameter of TFC membrane, leading to 40% improvement of water flux. Furthermore, the hybrid microporous membrane which was developed by doping SiO_2-GO nano hybrid exhibited nearly 2-fold increment in pure water flux with the rejection rate of albumin maintained at 98% (Wu et al., 2014).

Over the past several years, highly hydrophilic TiO_2 and GO nanomaterials are widely used in composite membrane fabrication. The unique properties of TiO_2 are high hydrophilicity, chemical stability, low toxicity and commercial availability (Emadzadeh et al., 2014; Yang et al., 2007). GO meanwhile offers desirable property with superior hydrophilicity due to the presence of abundant hydrophilic functional groups on its surface, i.e., hydroxyl, epoxide, carbonyl and carboxyl. Besides, GO is also associated with high surface area and great mechanical property (Lai et al., 2016a, 2016b; Zhang et al., 2010). It has been previously used as nanofiller in the selective layer synthesis of TFC membrane for the purpose of improving water permeability, anti-fouling and chlorine resistance (Chae et al., 2015). Previous reports demonstrated that the incorporation of TiO_2 or GO into the TFC substrate could improve the hydrophilicity and increase the support layer porosity enhancing the water flux (Emadzadeh et al., 2014; Park et al., 2015).

The main objective of this work is to study the effect of TiO_2/GO nanofillers on the properties of PSF substrate. The PSF nanocomposite substrates were further used for TFC membrane synthesis followed by process performance evaluation for FO applications. The study is of importance to give an insight into which nanofiller is better for nanocomposite substrate making as both nanofillers have been previously studied in separated work and were said to have positive improvement on PSF substrate.

2. Experimental

2.1. Material

Polysulfone Udel P-1700 in pellet form (PSF, Solvay Advanced Polymers), 1-methyl 1-2-pyrrolidinone (NMP, >99.5%, Merck) and polyvinylpyrrolidinone (PVP K30, Sigma-Aldrich) were used for TFC substrate synthesis. Commercial TiO_2 nanoparticles with particle size of <21 nm (Degussa P25, Evonik) and self-synthesized GO were used as nanofiller to prepare nanocomposite substrate. GO was synthesized using graphite powder (Sigma-Aldrich) according to Hummer's modified method. Sulfuric acid (H_2SO_4, 95–97%, Merck), sodium nitrate ($NaNO_3$, Riedel-de Haen), potassium permanganate ($KMnO_4$, >99%, Sigma-Aldrich) and hydrogen peroxide (H_2O_2, Riedel-de Haen) were used as the oxidizing agent to oxidize graphite powder to become GO. Barium chloride 2-hydrate ($BaCl_2{\cdot}2H_2O$, Riedel-de Haen), hydrochloric acid (HCl, 37%, Merck), acetone (RCl Labscan) and Milipore RO water (ASTM type III) were used for washing synthesized GO. 1,3-phenylendiamine (MPD, >99%, Merck), *n*-hexane (>99%, Merck) and 1,3,5-benzenetricarbonyl trichloride (TMC, >98%, Merck) were the monomers used for polyamide selective layer formation. Sodium chloride (NaCl, 99%, RCl Labscan) was used for salt solution preparation for RO and FO tests.

2.2. Flat sheet TFC FO membrane preparation

2.2.1. Substrate preparation

Table 1 shows the dope formulation used to prepare PSF substrate with and without nanofiller incorporation. To prepare the dope solution, PVP was first added into NMP and stirred for 10 min. It was followed by adding nanoparticles (TiO_2 or

Table 1 The composition of dope solutions and monomer solutions used for TFC membrane preparation.

TFC membrane	TiO_2:GO weight ratio	Composition of dope solution (wt%)				Aqueous and organic solution during IP process (wt/v%)	
		PSF	PVP	NMP	Nanofiller	MPD/water	TMC/*n*-hexane
$TFC_{control}$	–	17.50	0.50	82.00	–	2.00	0.10
TFC_{TiO_2}	1:0	17.41	0.50	81.59	0.50		
$TFC_{TiO_2/GO}$	0.5:0.5	17.41	0.50	81.59	0.50		
TFC_{GO}	0:1	17.41	0.50	81.59	0.50		

GO or mixture of TiO_2 and GO) into the solvent. PSF was then added into the mixture under vigorous stirring and the homogeneous dope solution produced was then ultrasonicated for 1 h to remove trapped air bubbles. The bubble-free dope solution was cast on the glass plate using glass rod followed by immediate immersion in a water coagulation bath at room temperature for phase inversion to take place. When the substrate was peeled off from the glass plate, it was transferred to another water bath and immersed for at least 24 h to remove solvent/PVP residual. At last, substrate with 70–90 μm of thickness was stored in pure water till use. The substrates produced are thereafter designated as $Substrate_{control}$, $Substrate_{TiO_2}$, $Substrate_{TiO_2/GO}$ and $Substrate_{GO}$, depending on the type of nanomaterials added.

2.2.2. Polyamide selective layer preparation

The selective layer of TFC membrane was formed by interfacial polymerization (IP) on the top surface of substrate. First, 30 mL of 2 wt/v% MPD aqueous solution was poured and held for 2 min to ensure the penetration of MPD solution into the substrate pores. The excess of MPD solution was then drained off and the residual was removed by soft rubber roller. Then, 30 mL of 0.1 wt/v% TMC in *n*-hexane was poured on the top of substrate surface and excess organic solution was drained off after 1 min contact time. The prepared TFC membrane was dried at ambient condition for 1 min followed by 8 min in an oven at 60 °C. At last, TFC membrane was stored in the pure water till use. These TFC membranes are thereafter called as $TFC_{control}$, TFC_{TiO_2}, $TFC_{TiO_2/GO}$ and TFC_{GO}, depending on the type of substrate chosen.

2.3. Membrane characterization

2.3.1. Substrate characterization

The functional groups of PSF substrate were identified by ATR-FTIR spectroscope (FTLA 2000 series, ABB). The scanning electron microscope (Quanta400, FEI) equipped with energy dispersive X-ray spectrometer (X-Max, Oxford) was used to study substrate morphology (surface and cross-section) and identify the atomic elements of top and bottom surface by silicon drift detector. The contact angle of both top and bottom surface of substrates was measured by the sessile drop technique using a contact angle goniometer (OCA 15 Pro, Data Physics). The surface roughness of substrates meanwhile was inspected by atomic force microscope (SPA-300 HV, Seiko).

2.3.2. Mass transport characteristics of substrate and TFC membrane

The pure water flux of substrates, water and salt permeabilities of TFC membranes were determined using RO experimental setup. The filtration cell used is dead-end stirred cell with effective membrane area of 14.62 cm^2. Nitrogen gas was used to achieve deasirable pressure. The deionized (DI) water (conductivity < 5 μs/cm) and NaCl aqueous solution with 1000 ppm were used as feed solution. Pure water flux (J), water permeability (A), salt rejection rate (R) and salt permeability (B) were calculated by the following equations (Chung et al., 2012; Emadzadeh et al., 2014; Lai et al., 2016a, 2016b):

$$J = \frac{m/\rho}{A_m \Delta t} \tag{1}$$

$$A = \frac{J}{\Delta P} \tag{2}$$

$$\frac{1-R}{R} = \frac{B}{A(\Delta P - \Delta \pi)} \tag{3}$$

$$R = \left(1 - \frac{C_p}{C_f}\right) \times 100 \tag{4}$$

where m is the mass of permeate water, ρ is the water density, A_m is the effective membrane area, Δt is the time, ΔP is the applied pressure difference, $\Delta \pi$ is the osmotic pressure difference, C_p and C_f are the salt concentration of the feed and permeate solution, respectively.

2.3.3. FO performance evaluation

The TFC membrane performance was further evaluated by FO setup. The FO experiment was carried out using cross-flow membrane cell with total effective membrane area of 29.75 cm^2. The feed and draw solution were circulated in counter-current mode using two peristaltic pumps with cross-flow velocity maintained at 0.025 m/s. Both feed and draw solution temperature were at ambient condition. The TFC membranes were tested with two different membrane orientations, i.e., PRO mode (active layer facing draw solution) and FO mode (active layer facing feed solution). Each experiment was performed for 30 min with triplication to yield average result. The membrane water flux was determined by weight changes of solution using digital weight balance that was placed under the draw solution tank. Solution conductivity was measured using conductivity meter (Mettler-Toledo). The conductivity was then converted to concentration using

Please cite this article in press as: Sirinupong, T. et al., Synthesis and characterization of thin film composite membranes made of PSF-TiO_2/GO nanocomposite substrate for forward osmosis applications. Arabian Journal of Chemistry (2017), http://dx.doi.org/10.1016/j.arabjc.2017.05.006

conductivity-concentration calibration curve. In the FO experiment, DI water was used as feed solution while NaCl aqueous solution with different concentrations (0.5 and 2 M) were used as draw solution. The FO water flux (J_w) and reverse salt (J_s) flux were calculated using the following equations (Emadzadeh et al., 2016):

$$J_w = \frac{\Delta m/\rho}{A_m \Delta t} \tag{5}$$

$$J_s = \frac{\Delta(C_t V_t)}{A_m \Delta t} \tag{6}$$

where Δm is the weight change of draw solution, ρ is the density of the feed solution, A_m is the effective membrane area, C_t and V_t are salt concentration and feed solution volume at the end of experiment, respectively and Δ_t is the measured time period.

2.3.4. Membrane structure parameter determination

The structural (S) parameter of TFC membrane is one of the support layer properties and can be defined by the membrane support layer thickness (l) and tortuosity (τ) over the porosity (ε). S value could be determined by fitting the FO experimental data using Eq. (7) for FO mode and Eq. (8) for PRO mode (Cath et al., 2013).

$$S = \frac{D}{J_w}\left[ln\frac{A\pi_{draw} + B}{A\pi_{feed} + J_w + B}\right] \tag{7}$$

$$S = \frac{D}{J_w}\left[ln\frac{A\pi_{draw} - J_w + B}{A\pi_{feed} + B}\right] \tag{8}$$

where D is the solute diffusion coefficient, π_{draw} and π_{feed} are the osmotic pressure of the feed and draw solutions, respectively.

3. Results and discussion

3.1. Substrate characterization

Fig. 1 presents the TEM images of nano-size commercial TiO_2 and self-synthesized GO. As can be seen, TiO_2 is quite different compared with the GO in terms of structure. TiO_2 is of spherical shape meanwhile GO is single flake form in nature. The impact of nanomaterials addition on the dope solution viscosity and PSF substrate properties with respect to surface contact angle (both top and bottom surface) and water permeability are summarized in Table 2. Overall, it was found that the viscosity of PSF dope solution increased upon addition of nano-material. With respect to hydrophilicity, the nanomaterial-embedded PSF substrates exhibited lower water contact angle compared to the pristine PSF substrate. For the membrane top surface, the nanomaterial-embedded PSF substrates showed contact angle between 68.4° and 70.5° while pristine PSF substrate displayed 73.1°. Further analysis revealed that the bottom surface of nanomaterial-embedded PSF substrates also showed lower contact angle (62.8–66.7°) in comparison to PSF substrate (69.2°). Comparing among three nanomaterial-embedded PSF substrates, it can be seen that $Substrate_{TiO_2}$ and $Substrate_{GO}$ displayed very similar contact angle for both top and bottom surfaces. $Substrate_{TiO_2/GO}$ meanwhile showed the lowest contact angle. The lowest contact angle of substrate normally would lead to greater water permeability owing to the improved surface hydrophilicity as reported elsewhere (Hu and Mi, 2013). However, we cannot completely rule out the changes in membrane pore size or cross-sectional morphology that lead to different water permeability for the nanocomposite substrates as $Substrate_{TiO_2}$ and $Substrate_{GO}$ exhibited very similar water contact angle. $Substrate_{TiO_2}$ and $Substrate_{GO}$ in this study showed pure water flux of 140.5 and 201.6 L/m^2 h, respectively.

Table 3 summarizes the values of three surface roughness parameters of the substrates. As can be seen, embedding inorganic nanomaterials into polymeric substrate increased the PSF substrate roughness for both top and bottom surfaces. It is very interesting to note that of the three nanomaterial-embedded PSf substrates prepared, all showed greater bottom surface roughness compared to their respective top surface roughness. The bottom surface roughness (in terms of R_a value) of $Substrate_{TiO_2}$, $Substrate_{TiO_2/GO}$ and $Substrate_{GO}$ were reported to be 28.71, 17.91 and 23.75 nm, respectively. These values were much higher compared to their respective top surface roughness, i.e., 19.09, 12.64 and 13.71 nm, respectively. The possible explanation for the rougher bottom surface for the nanomaterial-embedded PSF substrates was due to the presence of higher amount of nanomaterials on the bottom surface. This might happen during phase inversion process in

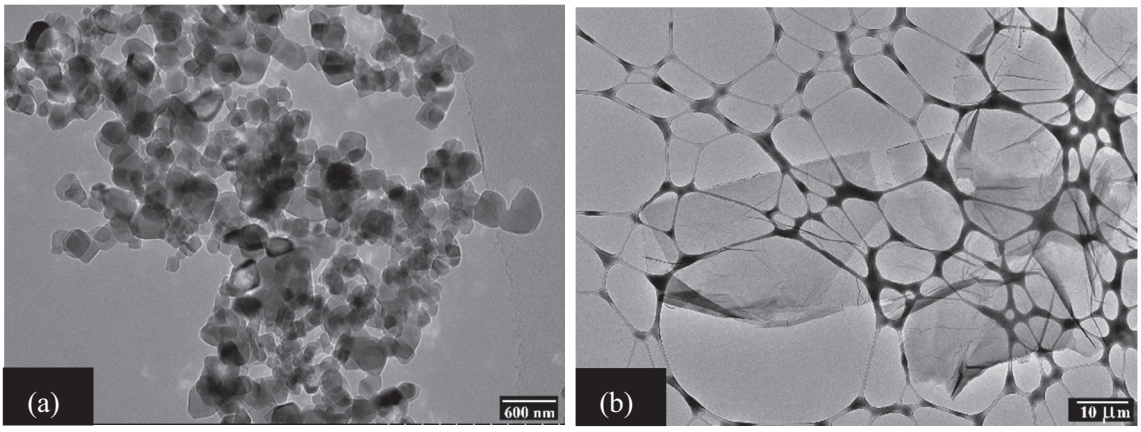

Figure 1 TEM images of (a) TiO_2 and (b) GO nanomaterial.

Table 2 Effect of TiO_2 and GO addition on the dope solution viscosity and properties of PSF substrates with respect to contact angle and pure water flux.

Substrate	Dope solution viscosity (mPa s)	Surface contact angle (°)		Pure water flux[a] (L/m^2 h)
		Top	Bottom	
$Substrate_{control}$	645.3	73.11 ± 2.18	69.15 ± 1.45	110.23 ± 0.88
$Substrate_{TiO_2}$	703.9	70.51 ± 2.27	65.19 ± 1.49	140.52 ± 1.79
$Substrate_{TiO_2/GO}$	731.5	68.39 ± 0.55	62.88 ± 1.19	297.65 ± 1.80
$Substrate_{GO}$	753.5	69.94 ± 1.34	66.66 ± 2.19	201.55 ± 1.91

[a] Pure water fluxes were measured by RO test at 2.5 bar, DI water as feed solution.

Table 3 Surface roughness of the PSF substrates via AFM analysis.

Substrate	Top surface[a]			Bottom surface[a]		
	R_a (nm)	R_{rms} (nm)	R_z (nm)	R_a (nm)	R_{rms} (nm)	R_z (nm)
$Substrate_{control}$	12.96	16.28	61.74	13.06	17.06	107.1
$Substrate_{TiO_2}$	19.09	24.60	74.32	28.71	27.02	157.0
$Substrate_{TiO_2/GO}$	12.64	16.38	61.01	17.91	22.53	77.05
$Substrate_{GO}$	13.71	17.40	47.48	23.75	29.41	121.1

[a] R_a: mean roughness, R_{rms}**:** root mean square of the Z value, R_z: mean difference between the highest peaks and lowest valleys.

Table 4 EDX results of PSF substrates with and without nanoparticle.

Substrate	Element of the top surface (wt%)				Element of the bottom surface (wt%)			
	Carbon	Oxygen	Sulfur	Titanium	Carbon	Oxygen	Sulfur	Titanium
$Substrate_{control}$	79.50	12.80	7.70	–	78.50	16.40	5.10	–
$Substrate_{TiO_2}$	77.90	16.00	5.20	0.90	76.55	14.15	7.55	1.75
$Substrate_{TiO_2/GO}$	78.55	14.30	6.45	0.70	77.15	19.85	2.80	0.20
$Substrate_{GO}$	79.00	12.90	8.10	–	78.05	18.05	3.90	–

which high-density nanomaterials tend to settle faster to the substrate bottom part.

The EDX results shown in Table 4 further justified the explanation. Overall, the bottom surface of $Substrate_{TiO_2/GO}$ and $Substrate_{GO}$ showed much higher oxygen (O) element compared with its top surface. The existing of more O amounts could be due to the chemical structure of GO and/or TiO_2 that consist of O element in the organic structure. Meanwhile for the $Substrate_{TiO_2}$, the increase in Ti element on the bottom surface could support the explanation that more nanomaterials were settled to bottom part of substrate during phase inversion process. The presence of more hydrophilic nanomaterials in the bottom surface of PSF substrate would be beneficial to minimize internal concentration polarization of TFC membrane during FO process. More discussion will be given in the following section.

Fig. 2 shows the SEM images of the top and bottom surface of nanocomposite PSF substrates together with their respective cross sectional morphology. Comparing between the top and bottom surface of four types of PSF substrates, it was found that the top surface contained much smaller pore size. This could be due to the formation of skin layer that was induced by phase inversion process. The presence of nodules on the top and bottom surface of PSF nanocomposite substrates could indicate the successful embedment of nanofillers throughout the substrate structure. From the cross section images, $Substrate_{TiO_2}$ and $Substrate_{TiO_2/GO}$ showed long finger-like voids extended from the top to the bottom, while $Substrate_{control}$ and $Substrate_{GO}$ showed short finger-like structure supported by macrovoid sublayer. The presence of hydrophilic nanofillers in the dope solution facilitates water diffusion to the polymer cast film, causing faster solvent (NMP) and non-solvent (water) exchange rate during phase inversion process and leads to formation long finger-like voids (Lai et al., 2017; Tang et al., 2010). The finger-like structure of $Substrate_{TiO_2/GO}$ was slightly wider and torturous than $Substrate_{TiO_2}$. This could be due to the synergistic effect of the increasing dope solution hydrophilicity and viscosity (Han and Nam, 2002; Vatanpour et al., 2011). However, it was observed that when only GO was used ($Substrate_{GO}$), the long finger-like structure as found in the $Substrate_{TiO_2/GO}$ was suppressed. The highest viscosity of PSF-GO dope solution as shown in Table 2 might have retarded the de-mixing process between solvent and non-solvent, leading to the macrovoid sublayer forming.

3.2. Characterization of TFC membranes

Table 5 summarizes three important properties of four different types of TFC membranes prepared in this work. They are

Please cite this article in press as: Sirinupong, T. et al., Synthesis and characterization of thin film composite membranes made of PSF-TiO_2/GO nanocomposite substrate for forward osmosis applications. Arabian Journal of Chemistry (2017), http://dx.doi.org/10.1016/j.arabjc.2017.05.006

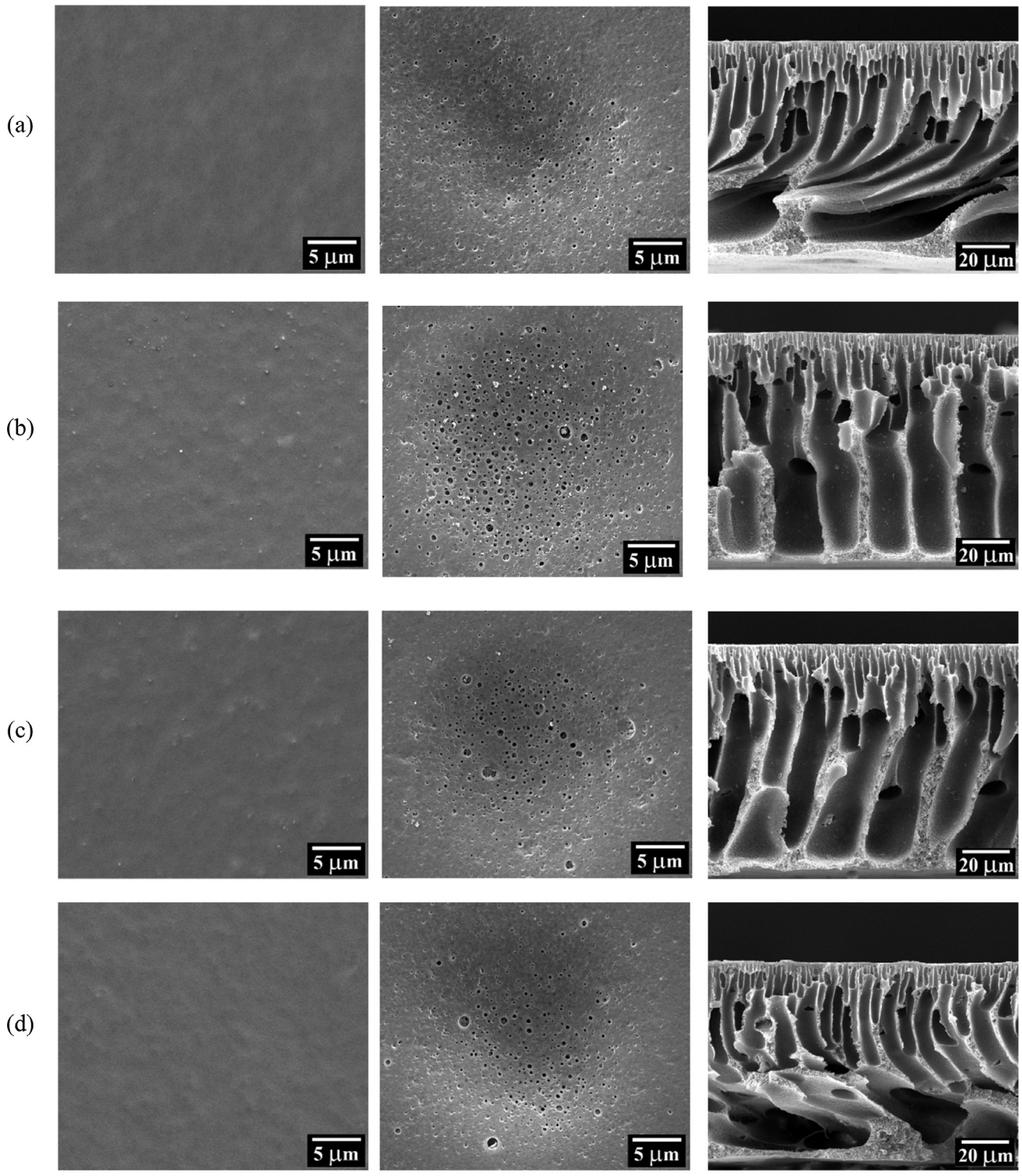

Figure 2 SEM images of top and bottom surface and cross section of PSF substrates prepared from different nanoparticle adding (a) Substrate (control), (b) $Substrate_{TiO_2}$, (c) $Substrate_{TiO_2/GO}$ and (d) $Substrate_{GO}$.

water permeability (A), salt permeability (B) and structural parameter (S). As shown, the A values of TFC membranes made of PSF nanocomposite substrates were in range of 1.5–1.7×10^{-12} m/s Pa. These values were 38–50% higher than the value shown by the $TFC_{control}$. The B values on the other hand displayed similar trend as A values, i.e., the higher the water permeability (A) the greater the salt permeability (B) and vice versa. In terms of S values, $TFC_{TiO_2/GO}$ showed the lowest value (0.20) followed by TFC_{TiO_2} (0.31), $TFC_{control}$ (0.37) and TFC_{GO} (0.42), respectively.

In general, the smaller the S value the better the support layer in minimizing internal concentration polarization during

Please cite this article in press as: Sirinupong, T. et al., Synthesis and characterization of thin film composite membranes made of PSF-TiO_2/GO nanocomposite substrate for forward osmosis applications. Arabian Journal of Chemistry (2017), http://dx.doi.org/10.1016/j.arabjc.2017.05.006

Table 5 Separation properties and S values of TFC membranes prepared from different PSF substrates.

Membranes	Water permeability[a], A		Salt permeability[b], B ($\times 10^{-8}$ m/s)	Structural parameter value[c], S (mm)
	(L/m^2 h bar)	($\times 10^{-12}$ m/s Pa)		
$TFC_{control}$	0.40 ± 0.01	1.12 ± 0.04	0.42 ± 0.15	0.37 ± 0.01
TFC_{TiO_2}	0.55 ± 0.02	1.55 ± 0.06	0.84 ± 0.07	0.31 ± 0.01
$TFC_{TiO_2/GO}$	0.58 ± 0.01	1.61 ± 0.05	1.44 ± 0.34	0.20 ± 0.01
TFC_{GO}	0.61 ± 0.01	1.69 ± 0.02	1.89 ± 0.07	0.42 ± 0.01

[a] Water permeabilities were measured by RO test at 10 bar and DI water as feed solution.
[b] Salt permeabilities were measured by RO test at 10 bar and 1000 ppm NaCl as feed solution.
[c] Structural parameter were evaluated by FO test at FO mode and DI water and 2 M NaCl as feed and draw solution, respectively.

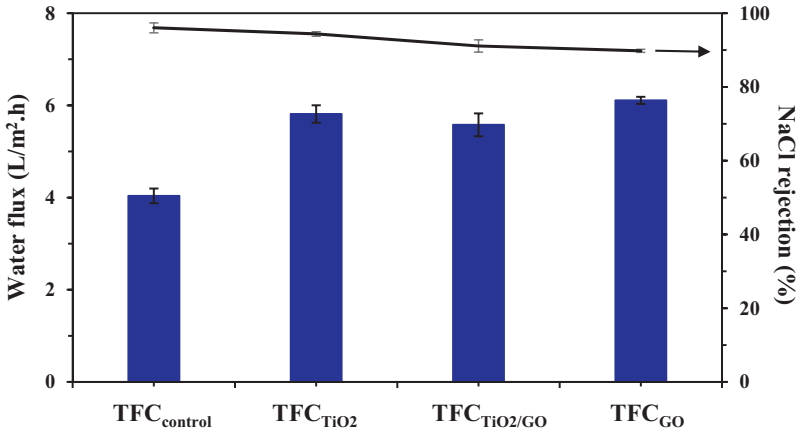

Figure 3 Water flux and NaCl rejection of TFC membrane prepared from PSF substrate incorporated with and without nanofiller (test condition: 10 bar at ambient temperature, feed solutions: 1000 ppm NaCl aqueous solution and DI water).

FO process leading to higher water permeate flux produced. The decrease in S value is corresponded to increase substrate porosity which could lead to faster mass transfer in membrane support layer (Hu et al., 2013; Huang and McCutcheon, 2015).

The effects of using nanofillers-embedded substrate on TFC membrane with respect to water flux and NaCl rejection were evaluated using dead-end RO experimental setup and the results are presented in Fig. 3. The $TFC_{control}$ exhibited 4.0 L/m^2 h and 96.0% salt rejection when it was tested at 10 bar using 1000 ppm NaCl aqueous solution. The water fluxes of TFC membranes made of nanocomposite substrates were in the range of 5–6 L/m^2 h. These values were 25–50% higher than that of $TFC_{control}$. This significant improvement could be due to the improved substrate hydrophilicity owing to the addition of TiO_2 and/or GO. However, high water permeability is not always associated with excellent salt rejection. In certain cases, the membrane salt rejection is compromised with high water flux. Salt rejection of membrane slightly decreased from 96.0% for $TFC_{control}$ to 94.4, 91.1 and 90.1% for TFC_{TiO_2}, $TFC_{TiO_2/GO}$ and TFC_{GO}, respectively. The decrease in salt rejection is probably due to the lower degree of cross-linked polyamide active layer formed over the rougher surface of nanomaterials-incorporated substrates (Gang, 2013). Substrates with rougher surface are likely to reduce the reaction rate between MPD and TMC monomer, forming a selective layer with larger pores. This as a consequence negatively affects the salt removal rate (but increases water flux) as experienced in this work. Similar results (i.e., salt rejection was slightly compromised with significant improvement in water flux) were also reported elsewhere in which zeolite and TiO_2 nanoparticles were introduced into the substrate (Emadzadeh et al., 2014; Ma et al., 2013).

3.3. Effect of nanomaterial embedding on the performance of TFC membrane during FO experiments

Fig. 4 presents the water flux of TFC membranes evaluated using cross-flow filtration setup performed using PRO mode and FO mode. The experiments were carried out using DI water as feed solution and 0.5 or 2 M NaCl as draw solution. As can be seen, the TFC_{TiO_2} and $TFC_{TiO_2/GO}$ exhibited higher water flux than that of $TFC_{control}$ regardless of membrane orientation and draw solution concentration. From Fig. 4(a), the water flux, using 0.5 M NaCl as draw solution, was significantly improved from 13.0 L/m^2 h ($TFC_{control}$) to 21.0 L/m^2 h ($TFC_{TiO_2/GO}$) in PRO mode from 5.9 L/m^2 h ($TFC_{control}$) to 12.3 L/m^2 h ($TFC_{TiO_2/GO}$) in FO mode upon addition of equal amount of TiO_2 and GO into the PSF substrate. Likewise, the $TFC_{TiO_2/GO}$ also showed greater water flux than the $TFC_{control}$ for the case where 2 M NaCl was used as draw solution (Fig. 4(b)). However, it must be noted that the water flux of membrane obtained from higher draw solution concentration was obviously greater than the membrane tested at lower draw solution concentration. This was primarily due to higher

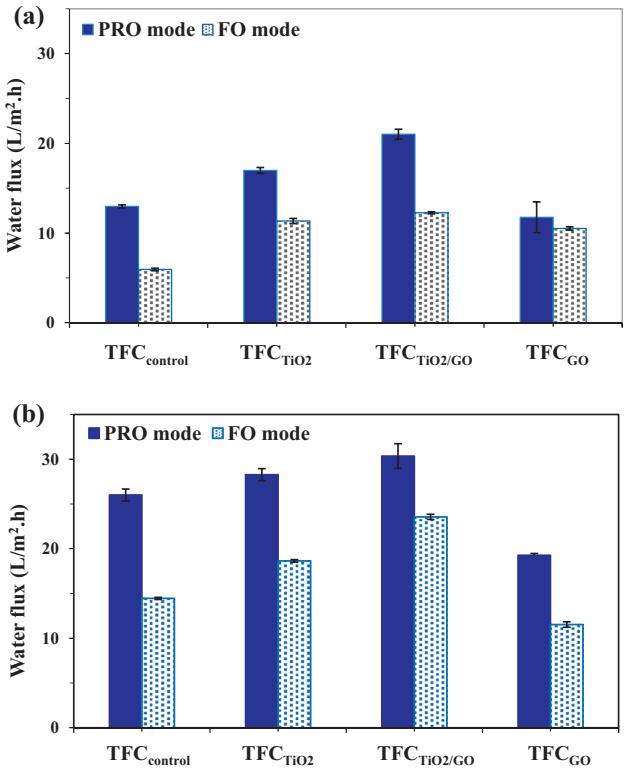

Figure 4 Water flux of TFC membrane prepared from PSF substrate and PSF nanocomposite substrate, (a) 0.5 M NaCl draw solution and (b) 2 M NaCl draw solution.

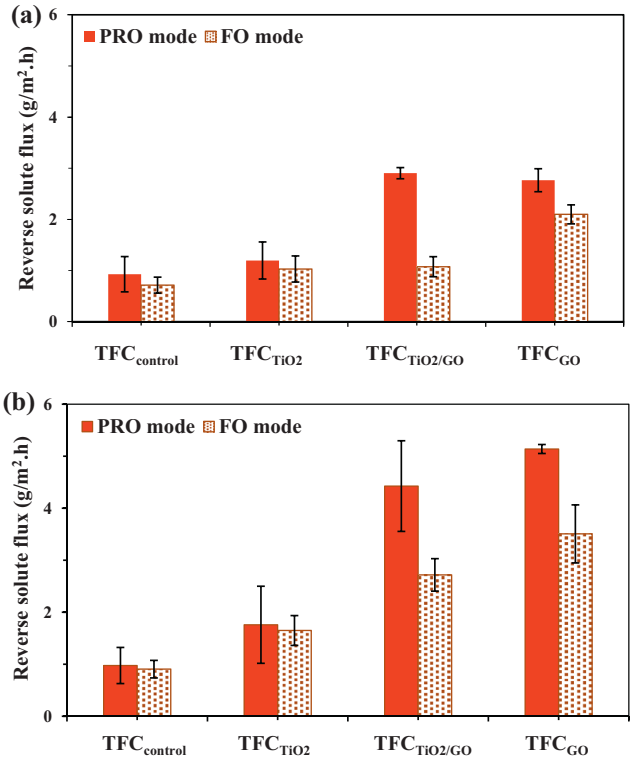

Figure 5 Reverse solute flux of TFC membrane prepared from PSF substrate and PSF nanocomposite substrate, (a) 0.5 M NaCl draw solution and (b) 2 M NaCl draw solution.

osmotic driven force created by higher concentration of osmotic agent solution. Compared with the water flux shown by TFC_{TiO_2} and $TFC_{TiO_2/GO}$, water flux of TFC_{GO} was reported to be much lower. Although all these three membranes were incorporated with hydrophilic nanomaterials, their substrate morphology was quite different. Unlike TFC_{TiO_2} and $TFC_{TiO_2/GO}$ membranes which possess longer finger-like structure (Fig. 2(b) and (c)), one can see that TFC_{GO} membrane displayed irregular microvoids at the bottom section of the substrate. The formation of such morphology is in fact not favorable for water transport. This, as a result, led to lower water flux as evidenced in this work.

Fig. 5 presents the reverse solute flux of the membranes tested with PRO mode and FO mode. Upon incorporation of nanomaterials into the PSF substrate, it was found that the resultant TFC membranes showed higher reverse draw solute flux compared with the control TFC membrane regardless of membrane orientation and draw solution concentration. Overall, TFC_{GO} showed the highest reverse draw solute flux followed by $TFC_{TiO_2/GO}$ and TFC_{TiO_2} and the reverse draw solute flux tended to increase with increasing the draw solution concentration. Although reverse solute flux of nanocomposite membranes was higher than that of control TFC membrane, it in fact had very minimal impact on the filtration performance as the values shown in this work were determined in the unit of g/m^2 h. This unit is much smaller in comparison to the unit of water flux, i.e., L/m^2 h (equivalent to kg/m^2 h) as shown in Fig. 4.

4. Conclusions

The effects of incorporating nanomaterials into PSF substrates on the properties of TFC membranes were investigated in this work. Both the surface properties of nanomaterials-embedded PSF substrate and its resultant TFC membrane were instrumentally characterized before proceeding to water filtration performance evaluation. The following are the highlights of the research work:

(a) The addition of nanomaterials in the PSF-based substrate has potential to increase the hydrophilicity of both top and bottom substrate surface as well as its surface roughness. In terms of water permeability at 2.5 bar, $Substrate_{TiO_2/GO}$ exhibited the highest pure water flux (297.7 L/m^2 h) followed by $Substrate_{GO}$ (201.6 L/m^2 h) and $Substrate_{TiO_2}$ (140.5 L/m^2 h). Control PSF substrate (Substrate) meanwhile showed only 110.2 L/m^2 h.

(b) The TFC membranes made of nanocomposite substrates in general showed much higher water flux (25–50%) compared with the control TFC membrane when tested in RO mode. Embedding nanomaterials into the PSF substrates only slightly affected the salt rejection of composite membranes as all the TFC membranes showed >90% NaCl rejection.

(c) Compared with the control TFC membrane, it was found that the TFC membranes made of $Substrate_{TiO_2}$ and $Substrate_{TiO_2/GO}$ showed higher water flux with no significant increase in reverse draw solute flux when all were tested under the same conditions using either PRO mode or FO mode.

Acknowledgements

This work is supported by the Thailand Research Fund under the Royal Golden Jubilee PhD Program (Grant No. PHD/0190/2557) and Graduate School, Prince of Songkla University, Thailand.

References

Cath, T.Y., Elimelech, M., McCutcheon, J.R., McGinnis, R.L., Achilli, A., Anastasio, D., Brady, A.R., Childress, A.E., Farr, I.V., Hancock, N.T., Lampi, J., Nghiem, L.D., Xie, M., Yip, N.Y., 2013. Standard methodology for evaluating membrane performance in osmotically driven membrane processes. Desalination 312, 31–38.

Chae, H.R., Lee, J., Lee, C.H., Kim, I.C., Park, P.K., 2015. Graphene oxide-embedded thin-film composite reverse osmosis membrane with high flux, anti-biofouling, and chlorine resistance. J. Membr. Sci. 483, 128–135.

Chung, K.Y.W., Chung, K.Y.W., Amy, G., 2012. Developing thin-film-composite forward osmosis membranes on the PES/SPSf substrate through interfacial polymerization. Am. Inst. Chem. Eng. 58, 770–781.

Chung, T.-S., Zhang, S., Wang, K.Y., Su, J., Ling, M.M., 2011. Forward osmosis processes: yesterday, today and tomorrow. Desalination 287, 78–81.

Cornelissen, E.R., Harmsen, D., de Korte, K.F., Ruiken, C.J., Qin, J. J., Oo, H., Wessels, L.P., 2008. Membrane fouling and process performance of forward osmosis membranes on activated sludge. J. Membr. Sci. 319, 158–168.

Deshmukh, A., Yip, N.Y., Lin, S., Elimelech, M., 2015. Desalination by forward osmosis: identifying performance limiting parameters through module-scale modeling. J. Membr. Sci. 491, 159–167.

Emadzadeh, D., Ghanbari, M., Lau, W.J., Rahbari-Sisakht, M., Matsuura, T., Ismail, A.F., Kruczek, B., 2016. Solvothermal synthesis of nanoporous TiO_2: the impact on thin-film composite membranes for engineered osmosis application. Nanotechnology 27 (345702), 1–12.

Emadzadeh, D., Lau, W.J., Matsuura, T., Rahbari-Sisakht, M., Ismail, a.F., 2014. A novel thin film composite forward osmosis membrane prepared from PSf-TiO_2 nanocomposite substrate for water desalination. Chem. Eng. J. 237, 70–80.

Gang, H., 2013. Development and fabrication of thin film composite (Tfc) membranes for engineered osmosis processes. J. Chem. Inf. Model. 53, 1689–1699.

Han, G., Zhang, S., Li, X., Widjojo, N., Chung, T.S., 2012. Thin film composite forward osmosis membranes based on polydopamine modified polysulfone substrates with enhancements in both water flux and salt rejection. Chem. Eng. Sci. 80, 219–231.

Han, M.J., Nam, S.T., 2002. Thermodynamic and rheological variation in polysulfone solution by PVP and its effect in the preparation of phase inversion membrane. J. Membr. Sci. 202, 55–61.

Hu, D., Xu, Z.L., Wei, Y.M., 2013. A high performance silica-fluoropolyamide nanofiltration membrane prepared by interfacial polymerization. Sep. Purif. Technol. 110, 31–38.

Hu, M., Mi, B., 2013. Enabling graphene oxide nanosheets as water separation membranes. Environ. Sci. Technol. 47, 3715–3723.

Huang, L., McCutcheon, J.R., 2015. Impact of support layer pore size on performance of thin film composite membranes for forward osmosis. J. Membr. Sci. 483, 25–33.

Kim, Y.C., Elimelech, M., 2013. Potential of osmotic power generation by pressure retarded osmosis using seawater as feed solution: analysis and experiments. J. Membr. Sci. 429, 330–337.

Lai, G.S., Lau, W.J., Goh, P.S., Ismail, A.F., Yusof, N., Tan, Y.H., 2016a. Graphene oxide incorporated thin film nanocomposite nanofiltration membrane for enhanced salt removal performance. Desalination 387, 14–24.

Lai, G.S., Lau, W.J., Gray, S.R., Matsuura, T., Gohari, R.J., Subramanian, M.N., Lai, S.O., Ong, C.S., Ismail, A.F., Emazadah, D., Ghanbari, M., 2016b. A practical approach to synthesize polyamide thin film nanocomposite (TFN) membranes with improved separation properties for water. J. Mater. Chem. A Mater. Energy Sustain. 4, 4134–4144.

Lai, G.S., Yusob, M.H.M., Lau, W.J., Gohari, R.J., Emadzadeh, D., Ismail, A.F., Goh, P.S., Isloor, A.M., Arzhandi, M.R.-D., 2017. Novel mixed matrix membranes incorporated with dual-nanofillers for enhanced oil-water separation. Sep. Purif. Technol. 178, 113–121.

Lau, W.J., Gray, S., Matsuura, T., Emadzadeh, D., Paul Chen, J., Ismail, A.F., 2015. A review on polyamide thin film nanocomposite (TFN) membranes: history, applications, challenges and approaches. Water Res. 80, 306–324.

Liu, X., Ng, H.Y., 2015. Fabrication of layered silica-polysulfone mixed matrix substrate membrane for enhancing performance of thin-film composite forward osmosis membrane. J. Membr. Sci. 481, 148–163.

Ma, N., Wei, J., Qi, S., Zhao, Y., Gao, Y., Tang, C.Y., 2013. Nanocomposite substrates for controlling internal concentration polarization in forward osmosis membranes. J. Membr. Sci. 441, 54–62.

Nayak, C.a., Rastogi, N.K., 2010. Forward osmosis for the concentration of anthocyanin from Garcinia indica Choisy. Sep. Purif. Technol. 71, 144–151.

Park, M.J., Phuntsho, S., He, T., Nisola, G.M., Tijing, L.D., Li, X.-M., Chen, G., Chung, W.-J., Shon, H.K., 2015. Graphene oxide incorporated polysulfone substrate for the fabrication of flat-sheet thin-film composite forward osmosis membranes. J. Membr. Sci. 493, 496–507.

Sahebi, S., Phuntsho, S., Woo, Y.C., Park, M.J., Tijing, L.D., Hong, S., Shon, H.K., 2016. Effect of sulphonated polyethersulfone substrate for thin film composite forward osmosis membrane. Desalination 389, 129–136.

Shaffer, D.L., Yip, N.Y., Gilron, J., Elimelech, M., 2012. Seawater desalination for agriculture by integrated forward and reverse osmosis: improved product water quality for potentially less energy. J. Membr. Sci. 415–416, 1–8.

Son, M., Choi, H., Liu, L., Celik, E., Park, H., Choi, H., 2015. Efficacy of carbon nanotube positioning in the polyethersulfone support layer on the performance of thin-film composite membrane for desalination. Chem. Eng. J. 266, 376–384.

Tang, C.Y., She, Q., Lay, W.C.L., Wang, R., Fane, A.G., 2010. Coupled effects of internal concentration polarization and fouling on flux behavior of forward osmosis membranes during humic acid filtration. J. Membr. Sci. 354, 123–133.

Tiraferri, A., Kang, Y., Giannelis, E.P., Elimelech, M., 2012. Super-hydrophilic thin-film composite forward osmosis membranes for organic fouling control: fouling behavior and antifouling mechanisms. Environ. Sci. Technol. 46, 11135–11144.

Vatanpour, V., Madaeni, S.S., Moradian, R., Zinadini, S., Astinchap, B., 2011. Fabrication and characterization of novel antifouling nanofiltration membrane prepared from oxidized multiwalled carbon nanotube/polyethersulfone nanocomposite. J. Membr. Sci. 375, 284–294.

Widjojo, N., Chung, T.S., Weber, M., Maletzko, C., Warzelhan, V., 2013. A sulfonated polyphenylenesulfone (sPPSU) as the supporting substrate in thin film composite (TFC) membranes with enhanced performance for forward osmosis (FO). Chem. Eng. J. 220, 15–23.

Wu, H., Tang, B., Wu, P., 2014. Development of novel SiO_2-GO nanohybrid/polysulfone membrane with enhanced performance. J. Membr. Sci. 451, 94–102.

Yang, Y., Zhang, H., Wang, P., Zheng, Q., Li, J., 2007. The influence of nano-sized TiO_2 fillers on the morphologies and properties of PSF UF membrane. J. Membr. Sci. 288, 231–238.

Please cite this article in press as: Sirinupong, T. et al., Synthesis and characterization of thin film composite membranes made of PSF-TiO_2/GO nanocomposite substrate for forward osmosis applications. Arabian Journal of Chemistry (2017), http://dx.doi.org/10.1016/j.arabjc.2017.05.006

Yin, J., Zhu, G., Deng, B., 2013. Multi-walled carbon nanotubes (MWNTs)/polysulfone (PSU) mixed matrix hollow fiber membranes for enhanced water treatment. J. Membr. Sci. 437, 237–248.
Zhang, K., Dwivedi, V., Chi, C., Wu, J., 2010. Graphene oxide/ferric hydroxide composites for efficient arsenate removal from drinking water. J. Hazard. Mater. 182, 162–168.
Zhu, J., Guo, N., Zhang, Y., Yu, L., Liu, J., 2014. Preparation and characterization of negatively charged PES nanofiltration membrane by blending with halloysite nanotubes grafted with poly (sodium 4-styrenesulfonate) via surface-initiated ATRP. J. Membr. Sci. 465, 91–99.

Please cite this article in press as: Sirinupong, T. et al., Synthesis and characterization of thin film composite membranes made of PSF-TiO_2/GO nanocomposite substrate for forward osmosis applications. Arabian Journal of Chemistry (2017), http://dx.doi.org/10.1016/j.arabjc.2017.05.006